

The Generalized Gibbs Ensemble (GGE) via the Hilbert space Monte Carlo sampling approach

Vincenzo Alba¹

¹International School for Advanced Studies (SISSA), Via Bonomea 265, 34136, Trieste, Italy, INFN, Sezione di Trieste
(Dated: July 9, 2015)

By combining *classical* Monte Carlo and Bethe ansatz techniques we devise a numerical method to construct the Truncated Generalized Gibbs Ensemble (TGGE) for the spin- $\frac{1}{2}$ isotropic Heisenberg (XXX) chain. The key idea is to sample the Hilbert space of the model with the appropriate GGE probability measure. The method can be trivially extended to other integrable systems, such as the Lieb-Liniger model. We benchmark our approach focusing on GGE expectation values of several local observables. The numerical results are in spectacular agreement with the Generalized Thermodynamic Bethe Ansatz (GTBA). Although the method is devised for finite-size chains, finite-size effects decay exponentially with system size, and moderately large chains are sufficient to extract thermodynamic quantities. Remarkably, it is possible to extract in a simple way the steady-state Bethe roots distributions, which encode complete information about the GGE expectation values in the thermodynamic limit. Finally, it is straightforward to simulate extensions of the GGE, in which, besides the integral of motion, one includes arbitrary functions of the Bethe-Gaudin-Takahashi roots.

Introduction.— The issue of how statistical ensembles arise from the out-of-equilibrium dynamics in *isolated* quantum many-body system is still a fundamental, yet challenging, problem. The main motivation of the renewed interest in this topic is the high degree of control reached in out-of-equilibrium experiments with cold atomic gases^{50–63}. The paradigm experiment is the so-called global *quantum quench*⁴, in which a system is initially prepared in an eigenstate $|\Psi_0\rangle$ of a many-body Hamiltonian \mathcal{H} . Then a global parameter of \mathcal{H} is suddenly changed, and the system is let to evolve unitarily under the new Hamiltonian \mathcal{H}' . At long times after the quench the system is expected to equilibrate, due to dephasing¹⁰ **more, Eisert?? la citazione e' a cazzo**, as confirmed by experiments **cite experiments**. On the other hand, in integrable models the presence of non-trivial *local* conserved quantities, besides the energy, strongly affects the dynamics and the nature of the steady state. As for now, it is still unclear whether such steady-state can be described by a statistical ensemble, and how to construct it.

Recently, it has been proposed that the stationary/equilibrium value of a generic local operator \mathcal{O} is described by a Generalized Gibbs Ensemble³ (GGE) as $\langle \mathcal{O} \rangle \equiv \text{Tr}(\mathcal{O} \rho^{GGE})$. Here ρ^{GGE} extends the Gibbs density matrix by including all the local conserved quantities \mathcal{I}_j (charges) as

$$\rho^{GGE} = Z^{-1} \exp(-\lambda_j \mathcal{I}_j). \quad (1)$$

Here, and in the rest of the paper, repeated indices are summed over. Z is a normalization factor. The λ_j are Lagrange multipliers to be fixed by imposing $\langle \Psi_0 | \mathcal{I}_j | \Psi_0 \rangle = \langle \mathcal{I}_j \rangle$, and $\mathcal{I}_2 = \mathcal{H}'$ is the post-quench Hamiltonian. In realistic situations one deals with the truncated GGE (TGGE), i.e., considering only a finite subset of the charges **citations**.

While the validity of the GGE has been largely confirmed in non-interacting field theories **cite papers**, in interacting ones the scenario is far less clear. For Bethe ansatz solvable models the so-called quench-action method⁴¹ **cite more** allows for an exact treatment of the steady state, provided that the overlap between the initial state $|\Psi_0\rangle$ and the eigenstates of \mathcal{H}' are known. Surprisingly, in several cases the quench-action is in disagreement with the TGGE **citations**, whereas it seems to

be supported by numerical simulations¹¹⁹. While one might argue that the GGE can be “repaired” by enlarging the set of charges included in (1), no quantitative study in this direction has been conducted yet **Is that true?**. One intriguing possibility is that local charges are not sufficient, and one has to include quasi-local ones¹²² **more citations**.

On the other hand, numerical methods, such as the time dependent density matrix renormalization group^{123,124} (tDMRG), have been mostly used to simulate the post-quench dynamics in microscopic models. However, no numerical attempt to explore the GGE itself has been undertaken yet. The aim of this work is to provide a Monte-Carlo-based framework for studying the GGE, and its possible extensions, in Bethe ansatz solvable models. Although we restrict ourselves to finite-size systems, thermodynamic quantities can be extracted by a standard finite-size scaling analysis. Moreover, finite-size corrections decay exponentially with system size, and moderately large systems are sufficient to access the thermodynamic limit. The method relies on the detailed knowledge of the Hilbert space structure provided by the Bethe ansatz formalism, and on the Bethe-Gaudin-Takahashi (BGT) equations **cite Takahashi book, revies**. The key idea is to sample the model Hilbert space according to the GGE probability measure given in (1). We should mention that the same idea has been already explored in Ref. 121 for the Gibbs ensemble. The method allows one to obtain GGE expectation value for generic observables, provided that their expression in terms of the roots of the BGT equations are known. Remarkably, it is also possible to extract the steady-state Bethe roots distributions, which encode the complete information about ensemble averages in the thermodynamic limit. It is also straightforward to extend the GGE including in (1) arbitrary functions of the Bethe roots, besides the \mathcal{I}_j . This could be useful, for instance, to investigate the effects of quasi-local charges **We should check how their expressions in terms of the rapidities look like**. Finally, we should mention that, in principle, GGE averages of local observables can be computed using exact diagonalization or Quantum Monte Carlo. However, both these methods require the operatorial expression of the conserved charges (see Re. 89 for the XXX chain), whereas our approach relies only on their expression

(typically simple) in terms of the BGT roots.

Here we perform a detailed benchmark of the approach focusing on the spin- $\frac{1}{2}$ isotropic Heisenberg chain (XXX chain), which is the venerable prototype of integrable models **cite Bethe and more**. We consider several TGGs (cf. (1)) constructed including $\mathcal{I}_2, \mathcal{I}_3, \mathcal{I}_4$, and varying the associated Lagrange multipliers λ_j . We focus on the conserved charges averages $\langle \mathcal{I}_j \rangle$ and their fluctuations $\sigma^2(\mathcal{I}_j) \equiv \langle \mathcal{I}_j^2 \rangle - \langle \mathcal{I}_j \rangle^2$. Both these quantities are related to well-known physical observables, such as the energy density, the energy current, the specific heat, and the thermal Drude weight **Cite something since it is non-trivial quantity**. We also compute the average magnetization and the spin susceptibility. Already for a chain with $L = 20$ sites the Monte Carlo data perfectly agree with the Generalized Thermodynamic Bethe Ansatz (GTBA) approach. We stress that this is the first direct numerical check of the GTBA for the XXX chain. Finally, we extract the BGT roots distributions for the Gibbs ensemble at several temperatures, and the GGE. In both cases finite-size effects are negligible for small roots, which are the relevant ones to describe the long-wavelength physics **I didn't check it properly but it is trivial**. For the Gibbs ensemble our findings are in perfect agreement with standard finite-temperature Thermodynamic Bethe Ansatz (TBA) results. **Why we are not doing it for the GGE?**

The-Heisenberg-spin-chain.— The isotropic spin- $\frac{1}{2}$ Heisenberg (XXX) chain with L sites is defined by the Hamiltonian

$$\mathcal{H} \equiv J \sum_{i=1}^L \left[\frac{1}{2} (S_i^+ S_{i+1}^- + S_i^- S_{i+1}^+) + S_i^z S_{i+1}^z \right], \quad (2)$$

where $S_i^\pm \equiv (\sigma_i^x \pm i\sigma_i^y)/2$ are spin operators acting on the site i , $S_i^z \equiv \sigma_i^z/2$, and $\sigma_i^{x,y,z}$ the Pauli matrices. We fix $J = 1$ and use periodic boundary conditions, identifying sites $L+1$ and 1. The total magnetization $S_T^z \equiv \sum_i S_i^z = L/2 - M$, with M number of down spins (particles), commutes with (2), and it is used to label its eigenstates.

In the Bethe ansatz formalism each eigenstate of (2) is univocally identified by M parameters $\{x_\alpha \in \mathbb{C}\}_{\alpha=1}^M$. In the thermodynamic limit $L \rightarrow \infty$ they form “string” patterns along the imaginary axis of the complex plane (string hypothesis) **cite Bethe Takahashi**. Strings of length $1 \leq n \leq M$ (n -strings) are parametrized as $x_{n;\gamma}^j = x_{n;\gamma} - i(n-1-2j)$. Here $x_{n;\gamma} \in \mathbb{R}$ is the string real part (string center), $j = 0, 1, \dots, n-1$ labels different string components, and γ denotes different string centers. The string hypothesis is not correct for finite chains, although deviations typically decay exponentially with L . Physically, the n -strings correspond to eigenstate components containing n -particle bound states. The $\{x_{n;\gamma}\}$ are the roots of the Bethe-Gaudin-Takahashi (BGT) equations

$$L\vartheta_n(x_{n;\gamma}) = 2\pi I_{n;\gamma} + \sum_{(m,\beta) \neq (n,\gamma)} \Theta_{m,n}(x_{n;\gamma} - x_{m;\beta}). \quad (3)$$

Here $\vartheta_n(x) \equiv 2\arctan(x/n)$, $\Theta_{m,n}(x)$ is the scattering phase between different roots, and $I_{n;\gamma} \in \frac{1}{2}\mathbb{Z}$ are the so-called

Bethe-Takahashi quantum numbers. The $I_{n;\gamma}$ satisfy the upper bound $|I_{n;\gamma}| \leq I_{\text{MAX}}(n, L, M)$, with I_{MAX} a known function of n, M, L ⁸⁶. Every choice of $I_{n;\gamma}$ identifies an eigenstate of (2). We define the “string content” of an eigenstate as $\mathcal{S} \equiv \{s_1, \dots, s_M\}$, with $0 \leq s_n \leq \lfloor M/n \rfloor$ the number of n -strings. The conserved charges \mathcal{I}_j of the XXX chain are given as

$$\mathcal{I}_{j+1} \equiv \frac{i}{(j-1)!} \frac{d^j}{dy^j} \log \Lambda(y) \Big|_{y=i}, \quad (4)$$

where Λ is the eigenvalue of the quantum transfer matrix $T(y)$ ⁹³, with y a spectral parameter. \mathcal{I}_2 is the XXX hamiltonian. The exact expression of the charges in terms of spin operators is known explicitly for $j \sim 10$ ⁸⁹. The support of \mathcal{I}_j , which is the number of sites where \mathcal{I}_j acts non trivially, increases linearly with j , i.e., larger j correspond to less local charges. The eigenvalues of \mathcal{I}_j on a generic eigenstate are obtained by summing the contributions of the different BGT roots *independently*. For instance, the energy is obtained as $E = 2 \sum_{n,\gamma} n/(n^2 + x_{n;\gamma}^2)$. Similar results are obtained for other charges using (4).

The-Hilbert-space-Monte-Carlo-sampling.— For a finite chain the GGE ensemble (1) can be simulated efficiently by sampling the eigenstates of (2) using Monte Carlo. One starts with an initial M -particle eigenstate, with string content $\mathcal{S} = \{s_1, \dots, s_M\}$, and identified by a BGT quantum number configuration $\mathcal{C} = \{I_{n;\gamma}\}_{n=1}^M$ ($\gamma = 1, \dots, s_n$). The corresponding charges eigenvalues are denoted as $\{\mathcal{I}_j\}$. Then a new eigenstate is generated with a Metropolis update. Specifically, each Monte Carlo step (mcs) consists of three moves:

1. Choose a new particle number sector M' , and string content \mathcal{S}' with probability $\mathcal{P}(M', \mathcal{S}')$.
2. Generate a new quantum number configuration \mathcal{C}' compatible with the \mathcal{S}' obtained in step 1. Solve the corresponding Bethe-Takahashi equations (3).
3. Calculate the charge eigenvalues \mathcal{I}'_j and accept the new eigenstate with the Metropolis probability:

$$\text{Min} \left\{ 1, \frac{L - 2M' + 1}{L - 2M + 1} e^{-\lambda_j(\mathcal{I}'_j - \mathcal{I}_j)} \right\}. \quad (5)$$

In (5) the factor in front of the exponential takes into account that \mathcal{I}_j are invariant under $SU(2)$ rotations **It is trivial from their eigenvalues**. Crucially, the steps 1 and 2 are necessary to account correctly for the density of states of the model, and are the same for the Gibbs ensemble¹²¹. The iteration of 1-3 defines a Markov chain, which, after some thermalization steps, generates eigenstates sampled according to (1). Clearly, it is straightforward to simulate the GGE with fixed particle number M . More interestingly, by trivially modifying (5) it is possible to simulate more exotic ensembles in which, in addition to \mathcal{I}_j , one considers arbitrary functions of the BGT roots. This could be useful to include the quasi-local charges in the *GGE*. Finally, the ensemble average $\langle \mathcal{O} \rangle$ of a generic

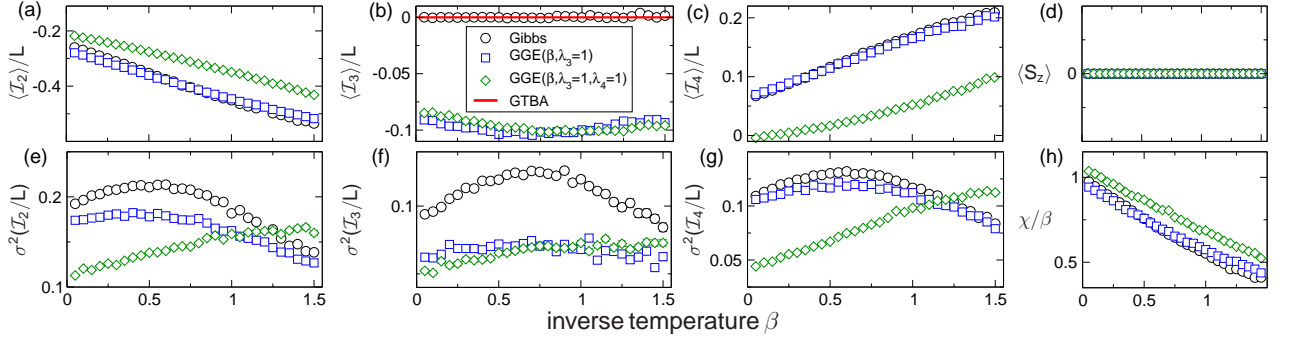


FIG. 1. The Generalized Gibbs Ensemble (GGE) for the Heisenberg spin chain with $L = 16$ sites: numerical results obtained using the Hilbert space Monte Carlo sampling. Only the first three conserved charges \mathcal{I}_n ($n = 1, 2, 3$), with associated Lagrange multipliers λ_n , are included in the GGE. Here \mathcal{I}_2 is the Hamiltonian and $\lambda_2 \equiv \beta$ the inverse temperature. In all the panels different symbols correspond to different values of λ_3, λ_4 . The circles correspond to the Gibbs ensemble, i.e., $\lambda_3 = \lambda_4 = 0$. (a) The GGE average $\langle \mathcal{I}_2 / L \rangle$ plotted as a function of β . (b) Variance of the GGE fluctuations $\sigma^2(\mathcal{I}_2 / L) \equiv \langle (\mathcal{I}_2 / L)^2 \rangle - \langle \mathcal{I}_2 / L \rangle^2$ as a function of β . (c)(d) and (e)(f): Same as in (a)(b) for \mathcal{I}_3 and \mathcal{I}_4 , respectively. In all panels the dash-dotted lines are the analytical results obtained using the Generalized Thermodynamic Bethe Ansatz (GTBA). (g) The GGE expectation value of the total magnetization $\langle S_z \rangle$. Notice that $\langle S_z \rangle = 0$ due to the $SU(2)$ invariance of the conserved charges. (h) χ / β plotted versus β , with χ being the magnetic susceptibility per site.

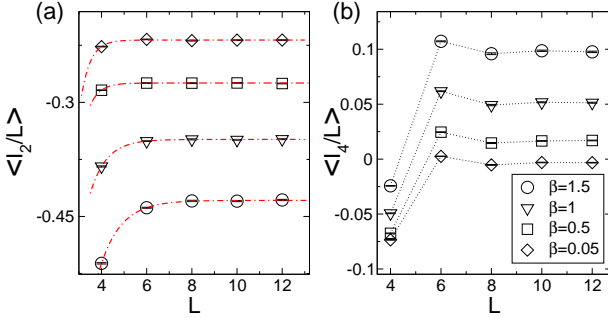


FIG. 2. Finite-size scaling of the GGE averages in the Heisenberg chain: Numerical results obtained from the Hilbert space Monte Carlo sampling. Here the GGE is constructed including $\mathcal{I}_2, \mathcal{I}_3, \mathcal{I}_4$, with Lagrange multipliers $\lambda_2 = \beta, \lambda_3 = \lambda_4 = 1$. (a) $\langle \mathcal{I}_2 / L \rangle$ plotted versus the chain size L for several values of β . The dash-dotted lines are exponential fits. (b) Same as in (a) for \mathcal{I}_4 .

operator is obtained as

$$\langle \mathcal{O} \rangle = \lim_{N_{\text{mcs}} \rightarrow \infty} \frac{1}{N_{\text{mcs}}} \sum_{|s\rangle} \langle s | \mathcal{O} | s \rangle, \quad (6)$$

where N_{mcs} is the total number of eigenstates $|s\rangle$ sampled in the Monte Carlo. For many local observables the contributions of the roots can be summed independently, i.e.,

$$\langle s | \mathcal{O} | s \rangle = \sum_{n, \gamma} f_{\mathcal{O}}(x_{n; \gamma}) \quad (7)$$

where the sum is over the BGT roots identifying the eigenstate $|s\rangle$, and $f_{\mathcal{O}}(x)$ depends on the observable. For the conserved charges \mathcal{I}_j the latter is obtained from (4).

The-GGE-for-local-observables.— The correctness of the Monte Carlo approach is illustrated in Fig. 1, considering the charge densities $\langle \mathcal{I}_j / L \rangle$ (panels (a)-(c) in the Figure), and the variance of their ensemble fluctuations $\sigma^2(\mathcal{I}_j / L) \equiv$

$\langle (\mathcal{I}_j / L)^2 \rangle - \langle \mathcal{I}_j / L \rangle^2$ (panels (e)-(g)). Panels (d)(h) plot the total magnetization $\langle S_z \rangle$ (i.e., the average particle number), and χ / β , with χ the spin susceptibility. Notice that $\langle \mathcal{I}_2 / L \rangle$ is the energy density, $\langle \mathcal{I}_3 / L \rangle$ the energy current, while $\sigma^2(\mathcal{I}_2 / L)$ and $\sigma^2(\mathcal{I}_3 / L)$ are related to the specific heat, and the thermal Drude weight, respectively. In all panels the data correspond to the TGGE constructed with the first three charges $\mathcal{I}_2, \mathcal{I}_3, \mathcal{I}_4$. Different symbols correspond to different values of the associated Lagrange multipliers, namely $\lambda_3 = \lambda_4 = 0$ (Gibbs ensemble, circles in the Figure), $\lambda_3 = 1$ and $\lambda_4 = 0$ (squares), and $\lambda_3 = \lambda_4 = 1$ (rhombi). All our results are plotted versus the inverse temperature $\lambda_2 = \beta$. The data are Monte Carlo results for $N_{\text{mcs}} = 5 \cdot 10^5$. In most of the cases, especially for small β the Monte Carlo error bars are small than the symbols. As expected, the different ensemble give different expectation values, implying that the local observables we consider are able to distinguish different GGEs. Notice that in panel (b) $\langle \mathcal{I}_3 \rangle = 0$ for the Gibbs ensemble due to the parity invariance of \mathcal{I}_j with even j , while in (d) $\langle S_z \rangle = 0$ due to the $SU(2)$ symmetry of (2). In all the panels in Fig. 1 the continuous lines are the analytic results obtained in the thermodynamic limit by solving the GTBA equations. These which fully match the Monte Carlo data, which signals that the finite-size effects are negligible already for $L = 16$, at least for the values of the λ_j considered.

The finite-size corrections are more carefully investigated in Fig. ?? . Fig. ?? plots $\langle \mathcal{I}_2 \rangle$ and $\langle \mathcal{I}_4 \rangle$ (panels (a) and (b), respectively) versus β . Here we focus on the TGGE with $\lambda_2 = \beta, \lambda_3 = 0$ and $\lambda_4 = 1$. Panel (a) demonstrates that finite-size effects decay exponentially with L for any β . Clearly, corrections are larger at lower temperature, as expected. Moreover, they increase with the range of the operator as shown in panel (b), although the behavior remains exponential.

Extracting-the-Bethe-roots-distributions.— In the thermodynamic limit in each n -string sector the roots of (3) become dense. Thus, each eigenstate is characterized by the

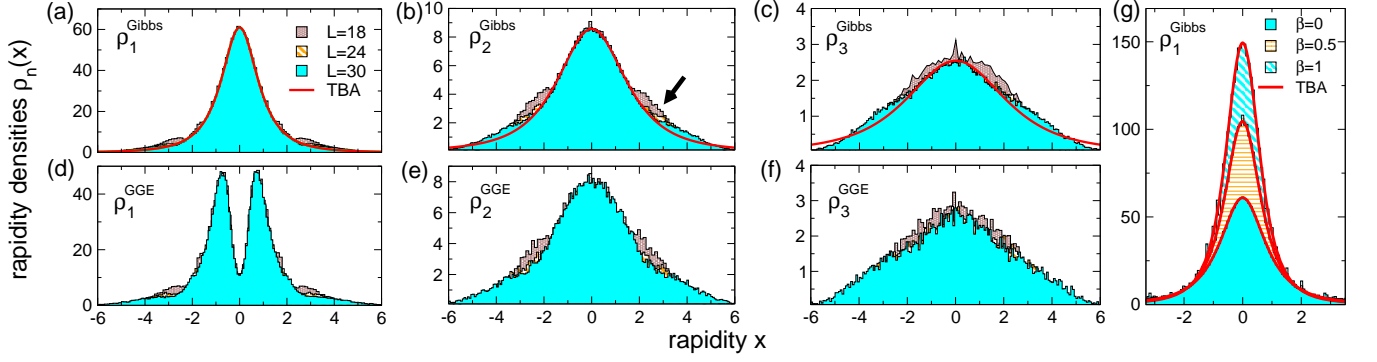


FIG. 3. The rapidity densities $\rho_n(x)$ (for $n = 1, 2, 3$) for the infinite temperature Gibbs (panels (a)-(c)) and the GGE equilibrium states (panels (d)-(f)): Numerical results for the Heisenberg spin chain obtained using the Hilbert space Monte Carlo sampling. Here the GGE is constructed including only \mathcal{I}_2 and \mathcal{I}_4 with fixed Lagrange multipliers $\lambda_2 = 0$ and $\lambda_4 = 1$. In all the panels the data are the histograms of the n -strings rapidities sampled in the Monte Carlo. The width of the histogram bins is $\Delta x = 2/L$. In each panel different histograms correspond to different chain sizes L . All the histograms are divided by 10^3 for convenience. In (b) the arrow is to highlight the finite-size effects. In panels (a)-(c) the lines are the Thermodynamic Bethe Ansatz (TBA) results. (g) Finite-temperature effects: Monte Carlo data for ρ_1^{Gibbs} for different values of the inverse temperature β .

root distribution $\rho \equiv \{\rho_n\}_{n=1}^\infty$. Formally, the ρ_n are defined as $\rho_n = \lim_{L \rightarrow \infty} [L(x_{n;\gamma+1} - x_{n;\gamma})]^{-1}$. For a generic observable \mathcal{O} , the GGE average becomes a functional integral as

$$\text{Tr}\{\exp(\lambda_j \mathcal{I}_j) \mathcal{O}\} \rightarrow \int \mathcal{D}\rho \exp(S[\rho] + \lambda_j \mathcal{I}_j[\rho]) \mathcal{O}[\rho]. \quad (8)$$

Here $S[\rho]$ is the Yang-Yang entropy. $S[\rho]$ counts the number of eigenstates leading to the same ρ , and it is extensive. In (8) \mathcal{O} is assumed that \mathcal{O} becomes a smooth function of ρ in the thermodynamic limit. Since both S and \mathcal{I}_j are extensive, the integral in (8) is dominated by the saddle point ρ^{sp} , with $\delta(S + \lambda_j \mathcal{I}_j)/\delta\rho|_{\rho=\rho^{sp}} = 0$. Here ρ^{sp} acts as a representative state for the ensemble, and it contains the full information about the GGE equilibrium steady state. Eq. (6) suggests/implies that the representative state root densities ρ_n^{sp} can be obtained the histograms of the roots $x_{n;\gamma}$ sampled in the Monte Carlo history, in the limit $L \rightarrow \infty$.

This is supported in Fig. 1 considering several GGEs. Panels (a)-(c) plot the root densities $\rho_n^{sp}(x)$ for $n = 1, 2, 3$ as a function of x for the representative state (saddle point) of the infinite-temperature Gibbs ensemble. In each panel the different histograms correspond to different chain sizes $18 \leq L \leq 30$. The data are obtained from Monte Carlo histories with $4 \cdot 10^5$ Monte Carlo steps. The width of the histogram bins is varied with the chain size as $2/L$. In all the panels the full lines are the analytic results obtained from the Thermodynamic Bethe Ansatz (TBA) (cf. (11)). Remarkably, the Monte Carlo data are in good agreement with the TBA results. This agreement is perfect for $n = 1$, whereas it becomes progressively worse upon considering larger $n > 1$ (see panels (b)(c)). Clearly, the deviations from the TBA result vanish upon increasing the system size (see for instance the arrow in panel (b)). These finite-size effects are larger on the tails of the distributions. This is expected since large rapidities correspond to large quasi-momenta, which are more sensitive to the lattice effects. Finally, finite-size effects increase with n ,

i.e., with the bound state sizes. The finite-temperature Gibbs ensemble is discussed in Fig. 1 (g), focusing on $\beta = 1/2$ and $\beta = 1$ (the different histograms in the panel). Only results for $\rho_1(x)$, for a chain with $L = 30$ are presented. The infinite temperature histogram is reported for comparison. The continuous lines are now the analytic results obtained by solving the finite-temperature TBA equations and perfectly agree with the Monte Carlo data. Upon lowering the temperature the height of the peak at $x = 0$ increases. This reflects that at $\beta = \infty$ the tail of the root distributions vanish exponentially, whereas for $\beta = 0$ they are $\sim 1/x^4$.

Finally, panels (d)-(f) plot $\rho_n(x)$ for the GGE ensemble. Specifically, we focus on the TGGE with the two charges $\mathcal{I}_2, \mathcal{I}_4$ with $\lambda_2 = 0$ and $\lambda_4 = 1$. In contrast with the thermal case (see (a)) ρ_1 exhibits a double peak structure. Similar to the infinite-temperature Gibbs ensemble ((a)-(c) in the Figure), the data suggest that for $L = 30$ finite-size effects are negligible, at least for $-2 \leq x \leq 2$.

I. CONCLUSIONS

II. THE STRING ROOT DENSITIES AT INFINITE TEMPERATURE

For infinite temperature the densities ρ_n are given as

$$\rho_n(x) = \frac{2}{\pi} \frac{1}{(n^2 + x^2)(x^2 + (2+n)^2)} \quad (9)$$

Notice that

$$\int_{-\infty}^{+\infty} \rho_n(x) dx = \frac{1}{n(n+1)(n+2)} \quad (10)$$

Including the first order correction to the infinite temperature result one obtains

$$\rho_n(x) = \frac{2}{\pi} \frac{1}{(n^2 + x^2)(x^2 + (2+n)^2)} - \frac{8}{\pi} \frac{n(n+2)}{(n^2 + x^2)^2(x^2 + (2+n)^2)^2} J\beta + \mathcal{O}(J^2\beta^2) \quad (11)$$

-
- ¹ M. Rigol, V. Dunjko, V. Yurovsky, and M. Olshanii, *Phys. Rev. Lett.* **98**, 050405 (2007).
- ² S. Popescu, A. J. Short, and A. Winter, *Nature Physics* **2**, 754 (2006).
- ³ M. Rigol, V. Dunjko, and M. Olshanii, *Nature* **452**, 854 (2008).
- ⁴ A. Polkovnikov, K. Sengupta, and M. Vengalattore, *Rev. Mod. Phys.* **83**, 863 (2011).
- ⁵ J. Eisert., M. Friesdorf, and C. Gogolin, arXiv:1408.5148.
- ⁶ C. Kollath, A. M. Läuchli, and E. Altman, *Phys. Rev. Lett.* **98**, 180601 (2007).
- ⁷ S. R. Manmana, S. Wessel, R. M. Noack, and A. Muramatsu, *Phys. Rev. Lett.* **98**, 210405 (2007).
- ¹²⁵ P. Calabrese and J. Cardy, *J. Stat. Mech.* P06008 (2007).
- ⁹ M. Cramer, C. M. Dawson, J. Eisert, and T. J. Osborne, *Phys. Rev. Lett.* **100**, 030602 (2008).
- ¹⁰ T. Barthel and U. Schollwöck, *Phys. Rev. Lett.* **100**, 100601 (2008).
- ¹¹ M. Cramer, A. Flesch, I. P. McCulloch, U. Schollwöck, and J. Eisert, *Phys. Rev. Lett.* **101**, 063001 (2008).
- ¹² M. Kollar and M. Eckstein, *Phys. Rev. A* **78**, 013626 (2008).
- ¹²⁶ A. Iucci and M. A. Cazalilla, *Phys. Rev. A* **80**, 063619 (2009).
- ¹⁴ S. Sotiriadis, P. Calabrese, and J. Cardy, *EPL* **87**, 20002 (2009).
- ¹⁵ G. Roux, *Phys. Rev. A* **79**, 021608 (2009).
- ¹⁶ M. Rigol, *Phys. Rev. Lett.* **103**, 100403 (2009).
- ¹⁷ M. Rigol, *Phys. Rev. A* **80**, 053607 (2009).
- ¹⁸ P. Barmettler, M. Punk, V. Gritsev, E. Demler, and E. Altman, *Phys. Rev. Lett.* **102**, 130603 (2009).
- ¹⁹ P. Barmettler, M. Punk, V. Gritsev, E. Demler, and E. Altman, *New J. Phys.* **12**, 055017 (2010).
- ²⁰ M. Cramer and J. Eisert, *New J. Phys.* **12**, 055020 (2010).
- ²¹ A. Flesch, M. Cramer, I. P. McCulloch, U. Schollwöck, and J. Eisert, *Phys. Rev. A* **78**, 033608 (2008).
- ²² G. Roux, *Phys. Rev. A* **81**, 053604 (2010).
- ²³ D. Fioretto and G. Mussardo, *New J. Phys.* **12**, 055015 (2010).
- ²⁴ G. Biroli, C. Kollath, and A. M. Läuchli, *Phys. Rev. Lett.* **105**, 250401 (2010).
- ²⁵ L. F. Santos and M. Rigol, *Phys. Rev. E* **82**, 031130 (2010).
- ²⁶ M. C. Bañuls, J. I. Cirac, and M. B. Hastings, *Phys. Rev. Lett.* **106**, 050405 (2011).
- ¹²⁷ P. Calabrese, F. H. L. Essler, and M. Fagotti, *Phys. Rev. Lett.* **106**, 227203 (2011).
- ²⁸ C. Gogolin, M. P. Mueller, and J. Eisert, *Phys. Rev. Lett.* **106**, 040401 (2011).
- ²⁹ M. Rigol and M. Fitzpatrick, *Phys. Rev. A* **84**, 033640 (2011).
- ³⁰ T. Caneva, E. Canovi, D. Rossini, G. E. Santoro, and A. Silva, *J. Stat. Mech.* (2011) P07015.
- ³¹ L. Santos, A. Polkovnikov, and M. Rigol, *Phys. Rev. Lett.* **107**, 040601 (2011).
- ³² A. C. Cassidy, C. W. Clark, and M. Rigol, *Phys. Rev. Lett.* **106**, 140405 (2011).
- ³³ F. H. L. Essler, S. Evangelisti, and M. Fagotti, *Phys. Rev. Lett.* **109**, 247206 (2012).
- ³⁴ M. A. Cazalilla, A. Iucci, and M.-C. Chung, *Phys. Rev. E* **85**, 011133 (2012).
- ³⁵ J. Mossel and J.-S. Caux, *New J. Phys.* **14** 075006 (2012).
- ³⁶ M. Rigol and M. Srednicki, *Phys. Rev. Lett.* **108**, 110601 (2012).
- ³⁷ J. Mossel and J.-S. Caux, *J. Phys. A: Math. Theor.* **45**, 255001 (2012).
- ¹³⁰ M. Fagotti and F. H. L. Essler, *Phys. Rev. B* **87**, 245107 (2013).
- ³⁹ M. Fagotti, *Phys. Rev. B* **87**, 165106 (2013).
- ¹³¹ M. Collura, S. Sotiriadis, and P. Calabrese, *Phys. Rev. Lett.* **110**, 245301 (2013).
- ⁴¹ J.-S. Caux and F. H. L. Essler, *Phys. Rev. Lett.* **110**, 257203 (2013).
- ¹³³ M. Kormos, A. Shashi, Y.-Z. Chou, J.-S. Caux, and A. Imambekov, *Phys. Rev. B* **88**, 205131 (2013).
- ⁴³ B. Bertini, D. Schuricht, and F. H. L. Essler, arXiv:1405.4813 (2014).
- ⁴⁴ S. Sotiriadis and P. Calabrese, *J. Stat. Mech.* (2014) P07024.
- ⁴⁵ F. H. L. Essler, S. Kehrein, S. R. Manmana, and N. J. Robinson, *Phys. Rev. B* **89**, 165104 (2014).
- ⁴⁶ M. Fagotti, M. Collura, F. H. L. Essler, and P. Calabrese, *Phys. Rev. B* **89**, 125101 (2014).
- ⁴⁷ M. Fagotti, *J. Stat. Mech.* (2014) P03016.
- ¹²⁰ B. Wouters, J. De Nardis, M. Brockmann, D. Fioretto, M. Rigol, and J.-S. Caux, *Phys. Rev. Lett.* **113**, 117202 (2014).
- ¹¹⁹ B. Pozsgay, M. Mestyán, M. A. Werner, M. Kormos, G. Zarànd, and G. Takács, *Phys. Rev. Lett.* **113**, 117203 (2014).
- ⁵⁰ M. Greiner, O. Mandel, T. Hänsch, and I. Bloch, *Nature (London)* **419**, 51 (2002).
- ⁵¹ T. Kinoshita, T. Wenger, and D. S. Weiss, *Nature (London)* **440**, 900 (2008).
- ⁵² S. Hofferberth, I. Lesanovsky, B. Fischer, T. Schumm, and J. Schmiedmayer, *Nature (London)* **449**, 324 (2007).
- ⁵³ I. Bloch, J. Dalibard, and W. Zwerger, *Rev. Mod. Phys.* **80**, 885 (2008).
- ⁵⁴ S. Trotzky, Y.-A. Chen, A. Flesch, I. P. McCulloch, U. Schollwöck, J. Eisert, and I. Bloch, *Nature Phys.* **8**, 325 (2012).
- ⁵⁵ M. Gring, M. Kuhnert, T. Langen, T. Kitagawa, B. Rauer, M. Schreitl, I. Mazets, D. A. Smith, E. Demler, and J. Schmiedmayer, *Science* **337**, 6100 (2012).
- ⁵⁶ M. Cheneau, P. Barmettler, D. Poletti, M. Endres, P. Schaua, T. Fukuhara, C. Gross, I. Bloch, C. Kollath, and S. Kuhr, *Nature (London)* **481**, 484 (2012).
- ⁵⁷ U. Schneider, L. Hackeruller, J. P. Ronzheimer, S. Will, S. Braun, T. Best, I. Bloch, E. Demler, S. Mandt, D. Rasch, and A. Rosch, *Nature Phys.* **8**, 213 (2012).
- ⁵⁸ M. Kuhnert, R. Geiger, T. Langen, M. Gring, B. Rauer, T. Kitagawa, E. Demler, D. Adu Smith, and J. Schmiedmayer, *Phys. Rev. Lett.* **110**, 090405 (2013).

- ⁵⁹ T. Langen, R. Geiger, M. Kuhnert, B. Rauer, and J. Schmiedmayer, *Nature Phys.* **9**, 640 (2013).
- ⁶⁰ F. Meinert, M. J. Mark, E. Kirilov, K. Lauber, P. Weinmann, A. J. Daley, and H.-C. Nagerl, *Phys. Rev. Lett.* **111**, 053003 (2013).
- ⁶¹ T. Fukuhara, A. Kantian, M. Endres, M. Cheneau, P. Schaua, S. Hild, C. Gross, U. Schollwöck, T. Giamarchi, I. Bloch, and S. Kuhr, *Nature Phys.* **9**, 235 (2013).
- ⁶² J. P. Ronzheimer, M. Schreiber, S. Braun, S. S. Hodgman, S. Langer, I. P. McCulloch, F. Heidrich-Meisner, I. Bloch, and U. Schneider, *Phys. Rev. Lett.* **110**, 205301 (2013).
- ⁶³ S. Braun, M. Friesdorf, S. Hodgman, M. Schreiber, J. Ronzheimer, A. Riera, M. del Rey, I. Bloch, J. Eisert, and U. Schneider, *arXiv:1403.7199*.
- ⁶⁴ J. M. Deutsch, *Phys. Rev. A* **43**, 2046 (1991).
- ⁶⁵ M. Srednicki, *Phys. Rev. E* **50**, 888 (1994).
- ⁶⁶ M. Srednicki, *J. Phys. A* **29**, L75 (1996).
- ⁶⁷ M. Srednicki, *J. Phys. A* **32**, 1163 (1999).
- ⁶⁸ S. Goldstein, J. L. Lebowitz, R. Tumulka, and N. Zanghi, *Phys. Rev. Lett.* **96**, 050403 (2006).
- ⁶⁹ S. Goldstein, J. L. Lebowitz, C. Mastrodonato, R. Tumulka, and N. Zanghi, *Proc. R. Soc. A* **466**, 3203 (2010).
- ⁷⁰ S. Goldstein, J. L. Lebowitz, R. Tumulka, and N. Zanghi, *Eur. Phys. J. H* **35**, 173 (2010).
- ⁷¹ T. N. Ikeda, Y. Watanabe, and M. Ueda, *Phys. Rev. E* **84**, 021130 (2011).
- ⁷² T. N. Ikeda, Y. Watanabe, and M. Ueda, *Phys. Rev. E* **87**, 012125 (2013).
- ⁷³ R. Steinigeweg, J. Herbrych, and P. Prelovšek, *Phys. Rev. E* **87**, 012118 (2013).
- ⁷⁴ W. Beugeling, R. Moessner, and M. Haque, *Phys. Rev. E* **89**, 042112 (2014).
- ⁷⁵ R. Steinigeweg, A. Khodja, H. Niemeyer, C. Gogolin, and J. Gemmer, *Phys. Rev. Lett.* **112**, 130403 (2014).
- ⁷⁶ S. Sorg, L. Vidmar, L. Pollet, and F. Heidrich-Meisner, *arXiv:1405.5404v2*.
- ⁷⁷ W. Beugeling, R. Moessner, and M. Haque, *arXiv:1407.2043*.
- ⁷⁸ V. Khemani, A. Chandran, H. Kim, and S. L. Sondhi, *arXiv:1406.4863*.
- ⁷⁹ H. Kim, T. N. Ikeda, and D. Huse, *arXiv:1408.0535*.
- ⁸⁰ L. Bonnes, F. H. L. Essler, and A. M. Läuchli, *arXiv:1404.4062* (2014).
- ⁸¹ J.-S. Caux and J. Mossel, *J. Stat. Mech.* (2011) P02023.
- ⁸² V. Alba, M. Fagotti, and P. Calabrese, *J. Stat. Mech.* (2009) P10020.
- ⁸³ N. Kitanine, J. M. Maillet, and V. Terras, *Nucl. Phys. B* **554**, 647 (1999).
- ⁸⁴ N. Kitanine, J. M. Maillet, and V. Terras, *Nucl. Phys. B* **567**, 554 (2000).
- ⁸⁵ L. Amico, R. Fazio, A. Osterloh, and V. Vedral, *Rev. Mod. Phys.* **80**, 517 (2008).
- ⁸⁶ M. Takahashi, *Thermodynamics of one-dimensional solvable models*, Cambridge University Press 1999.
- ⁸⁷ C. N. Yang and C. P. Yang, *J. Math. Phys.* **10**, 1115 (1969).
- ⁸⁸ M. Takahashi, *Prog. Theor. Phys.* **46**, 401 (1971).
- ⁸⁹ M. P. Grabowski and P. Mathieu, *Ann. Phys. N.Y.* **243**, 299 (1995).
- ⁹⁰ J. Eisert, M. Cramer, and M. B. Plenio, *Rev. Mod. Phys.* **82**, 277 (2009).
- ⁹¹ P. Calabrese, J. Cardy, and B. Doyon Eds., Special issue: Entanglement entropy in extended systems, *J. Phys. A* **42**, 50 (2009).
- ⁹² P. Calabrese and J. Cardy, *J. Phys. A* **42**, 504005 (2009).
- ⁹³ V. E. Korepin, N. M. Bogoliubov, and A. G. Izergin, *Quantum Inverse Scattering Methods and Correlation Functions*, Cambridge University Press 1997.
- ⁹⁴ X. Zotos and P. Prelovšek, *Phys. Rev. B* **53**, 983 (1996).
- ⁹⁵ H. Castella and X. Zotos, *Phys. Rev. B* **54**, 4375 (1996).
- ⁹⁶ X. Zotos, F. Naef, and P. Prelovšek, *Phys. Rev. B* **55**, 11029 (1997).
- ⁹⁷ F. C. Alcaraz, M. I. Berganza, and G. Sierra, *Phys. Rev. Lett.* **106**, 201601 (2011).
- ⁹⁸ I. Pizorn, *arXiv:1202.3336*.
- ⁹⁹ M. I. Berganza, F. C. Alcaraz, and G. Sierra, *J. Stat. Mech.* (2012) P01016.
- ¹⁰⁰ G. Wong, I. Klich, L. A. P. Zayas, and D. Vaman, *JHEP* **12** (2013) 020.
- ¹⁰¹ M. Storms, and R. R. P. Singh, *Phys. Rev. E* **89**, 012125 (2014).
- ¹⁰² R. Berkovits, *Phys. Rev. B* **87**, 075141 (2013).
- ¹⁰³ F. H. L. Essler, A. M. Läuchli, and P. Calabrese, *Phys. Rev. Lett.* **110**, 115701 (2013).
- ¹⁰⁴ M. Nozaki, T. Numasawa, T. Takayanagi, *Phys. Rev. Lett.* **112**, 111602 (2014).
- ¹⁰⁵ G. Ramirez, J. Rodriguez-Laguna, and G. Sierra, *arXiv:1402.5015*.
- ¹⁰⁶ F. Ares, J. G. Esteve, F. Falceto, and E. Sánchez-Burillo, *arXiv:1401.5922*.
- ¹⁰⁷ Y. Huang, and J. Moore, *arXiv:1405.1817*.
- ¹⁰⁸ T. Pálmai, *arXiv:1406.3182*.
- ¹⁰⁹ J. Mölter, T. Barthel, U. Schollwöck, and V. Alba, *arXiv:1407.0066*.
- ¹¹⁰ H.-H. Lai and K. Yang, *arXiv:1409.1224*.
- ¹¹¹ J. Sato, B. Aufgebauer, H. Boos, F. Göhmann, A. Klümper, M. Takahashi, and C. Trippé, *Phys. Rev. Lett.* **106**, 257201 (2011).
- ¹¹² M. Fagotti and P. Calabrese, *Phys. Rev. A* **78**, 010306 (2008).
- ¹¹³ V. Gurarie, *J. Stat. Mech.* (2014) P02014.
- ¹¹⁴ M. Collura, M. Kormos, and P. Calabrese, *J. Stat. Mech.* (2014) P01009.
- ¹¹⁵ M. Kormos, L. Bucciattini, and P. Calabrese, *EPL* **107**, 40002 (2014).
- ¹¹⁶ J.-S. Caux and J.-M. Maillet, *Phys. Rev. Lett.* **95**, 077201 (2005).
- ¹¹⁷ J.-S. Caux, R. Hagemans and J.-M. Maillet, *J. Stat. Mech.* P09003 (2005).
- ¹¹⁸ J.-S. Caux, *J. Math. Phys.* **50**, 095214 (2009).
- ¹¹⁹ B. Pozsgay, M. Mestyán, M. A. Werner, M. Kormos, G. Zaránd, and G. Takács, *Phys. Rev. Lett.* **113**, 117203 (2014).
- ¹²⁰ B. Wouters, M. Brockmann, J. De Nardis, D. Fioretto, M. Rigol, and J.-S. Caux, *Phys. Rev. Lett.* **113**, 117202 (2014).
- ¹²¹ S.-J. Gu, N. M. R. Peres, Y.-Q. Li, *Eur. Phys. J. B* **48**, 157 (2005).
- ¹²² E. Ilievski, M. Medejak, and T. Prosen, *arXiv:1506.05049*.
- ¹²³ S. R. White and A. E. Feiguin, *Phys. Rev. Lett.* **93**, 076401 (2004).
- ¹²⁴ A. J. Daley, C. Kollath, U. Schollock, and G. Vidal, *J. Stat. Mech.* (2004) P04005.
- ¹²⁵ P. Calabrese and J. Cardy, *J. Stat. Mech.* (2007) P06008.
- ¹²⁶ A. Iucci and M. A. Cazalilla, *Phys. Rev. A* **80**, 063619 (2009).
- ¹²⁷ P. Calabrese, F. H. L. Essler, and M. Fagotti, *Phys. Rev. Lett.* **106**, 227203 (2011).
- ¹²⁸ P. Calabrese, F. H. L. Essler, and M. Fagotti, *J. Stat. Mech.* (2012) P07016.
- ¹²⁹ P. Calabrese, F. H. L. Essler, and M. Fagotti, *J. Stat. Mech.* (2012) P07022.
- ¹³⁰ M. Fagotti and F. H. L. Essler, *Phys. Rev. B* **87**, 245107 (2013).
- ¹³¹ M. Collura, S. Sotiriadis and P. Calabrese, *Phys. Rev. Lett.* **110**, 245301 (2013).
- ¹³² M. Collura, S. Sotiriadis and P. Calabrese, *J. Stat. Mech.* (2013) P09025.
- ¹³³ M. Kormos, M. Collura and P. Calabrese, *arXiv:1307.2142*.

¹³⁴ G. Mussardo, Phys. Rev. Lett. **111**, 100401 (2013).